Characterization Physic-Mechanical and Fatigue of Date Palm Wood (Bechar-Algeria Region)

Ahmed Badraoui[1], Ali Chaoufi[2], Ali Benzegaou[3]

[1,2,3]Laboratory of Mechanics modeling and experimentation

Faculty of Technology, UNIVERSITY TAHRI MOHAMED OF BECHAR – ALGERIA

Received 03/10/ 2023; Accepted 05/01/ 2024; Published 19/01/2024

Abstract

Many researchers are currently looking into finding affordable alternative materials, taking advantage of natural waste or recycled materials. Among these resources, date palms stand out for their availability and durability. This study focuses on the physical and mechanical characterization and fatigue strength of the date palm trunk, with the aim of evaluating their potential for use as reinforcement in composite and insulating materials. The tests carried out are intended to determine the mechanical properties and fatigue strength of fibrous wood. The results obtained demonstrate a physical and mechanical characterization in accordance with the standards reported by the majority of researchers, while the fatigue tests reveal the capacity of the test pieces to withstand a defined number of cycles under a specific load.

Keywords: date palm trunk, physical and mechanical characterization, fatigue.

Tob Regul Sci.™ 2024;10(1): 1862 - 1877

DOI: doi.org/10.18001/TRS.10.1.117

1. Introduction

Advances and developments in industry, especially in building materials, have led many researchers to focus on green construction and to take advantage of available but under-exploited renewable resources. Date palms are among these sources that generate large quantities of dry palms each year, in the form of waste resulting from their natural growth and development [1].

The so-called bio-source materials are used in various fields such as thermal insulation, industry, construction and packaging. Their interest lies in their mechanical, physical and thermal properties, which are also present in other plant materials used for composites, such as jute[2], flax[3], kernaf [4],[19], hemp[5], ramie[6], abaca[7], sisal[8], and others. In addition, they offer undeniable economic and environmental benefits. [9]

Some researchers have used date palm fibers as reinforcement in composite materials, with promising results under different loads [17], [18]. In addition, date palms are proving to be a good candidate for thermal insulation of buildings at room temperature, offering efficient and safe solutions [10].

The incorporation of date palm fibers as reinforcement in composite materials increases their resistance to thermal degradation, starting at 232 °C [11]. Dry fibers also have a tensile strength and a Young's modulus 10 to 20% higher than wet fibers [12].

Around the world, date palm fibers are among the most produced, exceeding coconut fiber by 42% and sisal and hemp by 10-20% respectively [13]. In addition, the use of petiole and date palm spine as reinforcement in gypsum and mortar composites allows their thermal conductivity and mechanical properties to be studied [14], [15].

Despite the growing interest in bio-source materials, few studies have investigated their fatigue behavior. The aim of this study is to examine the fatigue of the date palm trunk, starting with its physical and mechanical characterization, before determining its ability to withstand cyclic fatigue stresses.

2. Materials and method

2.1. Materials

The trunk of the date palm of the Feggous type, originating from the Béchar region of Algeria, has a unique and remarkable characteristic: it is devoid of twigs and is crowned with a coronary structure called stipe. This stipe ends with a single terminal bud, surrounded by leaves called palms or slingshots. Typically cylindrical, the trunk is dried naturally for at least two years, which gives it a particular structure. It consists of petiole fibers that intertwine with each other from the inside to the outside, ensuring its strength and strength.

Figure1. Date palm (a), Trunk (b), trunk cutting (c)

2.1.1 Trunk morphology

Figure 1 shows the morphological structure of the trunk wood in three sections along the direction of the blade axis: cross section (CT), and a longitudinal section (CL). It is observed that the size of the trunk section is constant throughout the date palm and that the direction of the fibres follows the direction of the section with a reduction in their section. Microscopic observation of the trunk cross-section shows the concentration of fibres relative to that of the plant matrix.

Figure 2 shows a longitudinal section of part of the wood of the trunk with a cross-section of 5×5 cm². Microscopic observation of cross-sections (CT) of different trunk areas from the same line along the trunk, Figure 3, shows that the fiber section and trunk percentage.

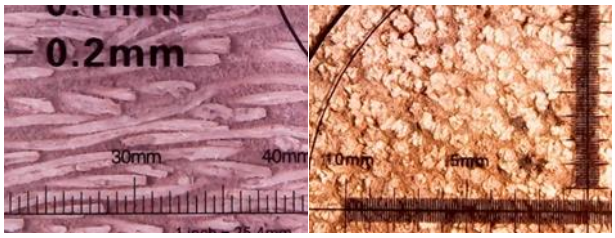

Figure2. Longitudinal section Figure 3. Cross section

2.2. Methods

2.2.1. Preparation of the Trunk Test Pieces

A fragment of the trunk of the date palm, as illustrated in Figure 1, is taken for analysis. Using a mechanical saw, the trunk is cut longitudinally, and then the plate is cut using a machine tool equipped with a diamond disk, figure 4. This plate is used to manufacture different test pieces for bending, tensile, compression and fatigue tests, as shown in figure 5.

Figure 4. Cutting the Test specimen (a) traction, (b) compression, (c) fatigue

Figure 5. Test peciment for bending, traction, compression and fatigue.

2.2.2. Physic-mechanical characterization and trunk fatigue

A. Physical properties

A.1. Drying technique:

The trunk plates are immersed in a tank of water for a period of seven days, and then thoroughly cleaned with distilled water to remove any impurities. They are then dried in an oven at a temperature of 60° C. until their mass stabilizes, as indicated in figure 6.

The objective of this drying process is to reduce the water content present in the internal structure of the wood. This method was applied to all specimens to ensure standardized conditions for future testing.

Figure 6. Drying of test pieces

A.2 Humidity H:

The moisture contents His determined from the following formula:

$$H\% = \frac{(M_h - M_s)}{M_h} x100 \qquad (1)$$

H %: percentage of water in the wood.

Mh: mass of sample before drying.

Ms: mass of sample after drying.

A.3. Density

The mass m, alone, does not tell about the nature of the body. Likewise, the volume V does not give any information on the nature of the body. But the quotient is a constant that characterizes the pure body; it is its density.

Thus, the density of a homogeneous substance is the mass of one unit of volume.

$$\rho = \frac{m}{v} Kg/m^3 \qquad (2)$$

It is expressed in SI units in $kg.m^{-3}$.

Or else $\rho_{apparant} = \frac{M_0}{(v_2 - v_1) - \frac{M - M_0}{\rho_{paraffine}}}$ (3)

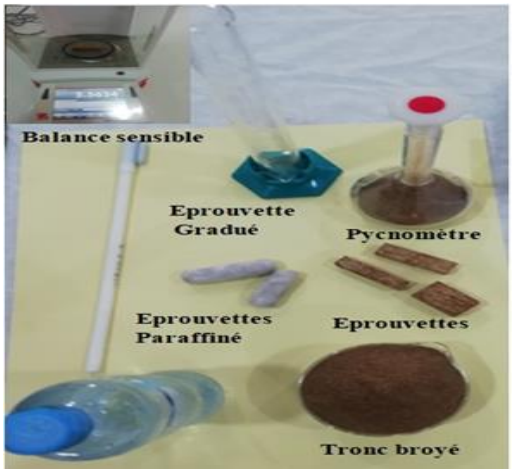

Figure 7. Measurement of trunk volume and mass

With: ρparaffin =850 Kg/m3, M0: mass of the sample, M: mass of the paraffin zed sample,v1: volume of the test piece filled with water, v2: new volume with submerged paraffin zed sample.

$$\rho_{absolue} = \frac{P_1 - \rho_{eau}}{P_2 - P_3} \qquad (4)$$

With: P1: sample weight, P2: weight of powder-filled pycnometer, P3: weight of water-filled pycnometer.

Usual units: g.cm^{-3}; kg. L^{-1} (1 g.cm^{-3} = 1 kg. L^{-1} = 1000 kg.m^{-3})

A.4 Density

The density of the wood is calculated by taking the same volume of the substance and water and measuring two masses and then the ratio of the mass of the substance Ms to the mass of the water Me is calculated

$$d = \frac{s}{e} = \frac{\rho_s}{\rho_e} \qquad (5)$$

Where:ρ_s: density of the substance, ρ_e: density of the water

B. Mechanical property

The test bench used GUNT50 KN with direct force generating hydraulic drive. The test force and elongation of the test pieces shall be measured by sensors and displayed. The measurement values are transmitted to a PC for evaluation using the software provided [10].

The fiber tensile examination is performed on test equipment called ESSOM, as illustrated in Figure 14. The speed of movement of the jaws is adjusted to 0.1 mm/min and the fibres are clamped between two jaws provided with rubber to prevent sliding.

The third ESSOM equipment is used to study the effects of fatigue using a rotating cantilever sample.

The fatigue test bench uses a spindle specimen and is attached to one end of a rotating shaft held at the base by self-aligned bearings. The load is applied to the pin producing a sinusoidal bending stress. The digital revolution counter takes into account the number of revolutions in case of failure.

2.2.3. Mechanical tests

A. Trunk pulling test

The test pieces of the tensile tests are dumbbell-shaped according to the standard NF ISO 527. The position of the fibres is longitudinal in figure 9. The ends of the test pieces shall be covered with green paper to prevent the test piece from sliding and crushing during the test in Figure 5. The test speed is of the order of 2 mm/min.

B. Compression test

The compression test was carried out on (30×30×30) mm 3 test pieces in the longitudinal and transverse direction of figure 10 according to NF standard B51-007-ISO3132-1975. The test speed is constant at a value of 5 mm/min.

C. Three-point bending test

The three-point static bending test is carried out according to ISO 178 on test pieces of dimensions (140×15×7) mm3. The speed of the test is of the order of 2 mm/min. Figure 12. By using the load-displacement curves obtained by the three-point bending test, the modulus of elasticity in bending Ef can be determined according to formula (6) under the standard (NFT 51 001). The bending strain ε and the bending stress σ are determined respectively according to formulae (7) and (8).

$$E_f = \frac{L^3 F}{4bh^3 s} \quad (6)$$

$$\varepsilon = \frac{6hs}{L^2} \quad (7)$$

$$\sigma = \frac{3FL}{2bh^2} \quad (8)$$

F: applied load (N), b: thickness of test peciment (mm), L: distance between supports (mm),

s: flexion obtained by the load (mm), h: test peciment height (mm).

D. Fiber tensile test

The tensile tests are carried out on the fibres taken from the wood of the trunk, in accordance with NI EN ISO 5079. The cross-section of the wood, shown in figure 3, shows that the fibres have a diameter of d=0.6 mm. The cross-section of the fibres remains constant over their entire length, which facilitates the direct estimation of the modulus of elasticity E and of the maximum stress σmax during the calculations.

E. Fatigue Test

The cyclic fatigue test in Figure 16 is performed on cylindrical test pieces in Figure 18. The load of the test is of the order of 5 %. From the results of the test, the Wöhler curve is plotted to show the behavior of the material in the cyclic fatigue range. It defines a relationship between the amplitude stress σa and the number of cycles at break Nr.

Alternating Stress:

$$\sigma_a = \frac{FL}{(\frac{\pi d^3}{32})} \quad (10)$$

With:

F = the applied force.

l = Length of test section = 102 mm

d = diameter of test piece = 8 mm

Type of test piece: Bio composites. Tare load: 30 kg

Diameter of test piece: 8 mm Stress: 100.396 N/mm2

3. Results and discussion

3.1 Physical property

3.1.1 Moisture content

The results of the drying process are presented in Table 1, showing the measurements in the natural and wet state of a test piece (30×30×30) mm3.

Table 1.

Natural mass (g)	The wet mass (g)	The mass after drying (g)
15.6	21.3	10.57

The moisture contents His determined from formula (1):

$$H\% = \frac{(21.3 - 10.57)}{21.3} x100$$

$$H\% = 50.37\%$$

3.1.2 Density

To calculate the absolute density, a part of the trunk is crushed and screened, less than 0.1 mm. A quantity of 20 g is taken.

P_1 = 20g, P_2 = 362.11g, P_3 = 358.15g et $\rho_{eau} = 1000Kg/m^3$

$\rho_{absolue} = 28191.91\ Kg/m^3$

The apparent density is calculated by equation (3)

$\rho_{apparent} = 687.9488Kg/m^3$

Density is the ratio of apparent density to water density

$$d = \frac{\rho_{absolue}}{\rho_{eau}} = \frac{687.9488}{1000} = 0.6879$$

3.2 Mechanical properties

3.2.1. Trunk tensile test

Figure 8 represents the tensile test of the test pieces of the trunk, the results are illustrated by the stress-strain curve, as shown in figure 9. This curve initially has a linear phase in which the stress applied is proportional to the strain undergone. Next, a steep drop in the curve is observed, marking the beginning of a more significant deformation, until the rupture of the test piece occurs.

In Table 2, the mean stress values associated with the mean deformation E % for the three test pieces can be observed. Remarkably, these values are very similar and convergent towards the same result for Young's modulus.

Results of the tensile test

Figure 8. Longitudinal tensile test

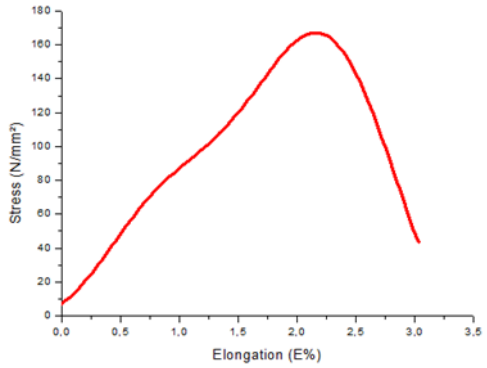

Figure 9. Stress assessment based on Deformation

Table2. Results of the longitudinal tensile test

σmax [MPa]	E(%)	E [MPa]
172.5	1.88	8625

Transverse traction is impractical because of the orientation of the fibres, which are short. In this context, the application of the load would be perpendicular to the alignment of the fibres, which would result in easy rupture of the test pieces.

3.2.2. Compression test

The results of the longitudinal and transverse compression test are shown in figure 10, where the load-displacement curves demonstrate an initial linear behavior, followed by a continuous decrease until the specimens (longitudinal and transverse) of the trunk reach their maximum deformation and rupture, as illustrated in figure 11.

Table 3 summarizes the results of the tests (longitudinal and transverse) by providing the max value of the stress associated with the deformation E%, as well as the corresponding value of the Young's modulus.

Results of the compression test

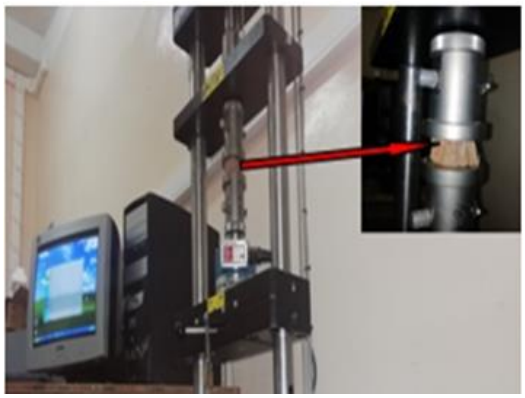

Figure10. Longitudinal and transverse compression test

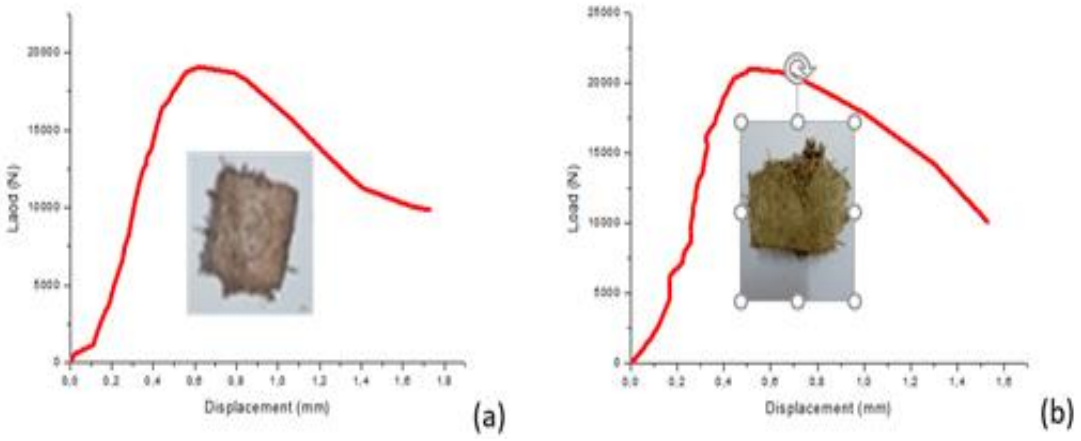

Figure 11. Stress Evaluation – Strain(a) Longitudinal, (b) transverse

Table 3. Results of the compression test

a-Longitudinal

σmax [MPa]	E(%)	E_L [MPa]
21.22	2.44	312.05

b- Transverse

σmax [MPa]	E(%)	E_T [MPa]
23.33	2	353.33

3.2.3. Three-point bending test

The load-displacement graph, as shown in Figure 13, is generated from the three-point bending tests shown in Figure 12. This graphical representation shows an initial phase in which the load displacement relationship is linear and elastic until the load reaches 200N, followed by a gradual decrease until breaking.

In Table 4, the average results of the tests carried out on three test pieces are summarized. This data highlights the relationship between maximum load and maximum displacement, as well as the value of Young's modulus associated with these tests.

Results of the three-point bending test

Figure 12. Three-point bending tests

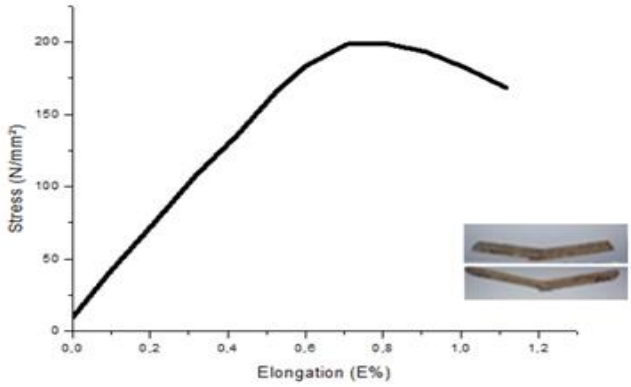

Figure 13. Stress Evaluation – Strain

Table 4. Results of the three-point bending tests

Fmax[N]	σmax [MPa]	dL (mm)	$E_f$max [GPa]
800	163.26	2.44	16

Table 5. Comparison of mechanical properties of date palm woods

	Modulus of elasticity [GPa]	Max Stress [MPa]	Region	References
	$16^{(F3P)}$	$163.26^{(F3P)}$		
	$0.31^{(CL)} – 0.35^{(CT)}$	$21.22^{(CL)}$- $23.33^{(CT)}$	Bechar	This study
	$1.43^{(TL)}$	$17.25^{(TL)}$		
Trunk of palm tree	$3,87^{(TL)}$	$95,35^{(TL)}$	Borj-rose Biskra-Algeria	[14]

$9{,}8^{(TL)}$	$35^{(TL)}$		
$0{,}1^{(CT)}$ _$2{,}2^{(CL)}$	$5^{(CT)}$_$35^{(CL)}$	Biskra-Algeria	[43]
$8{,}5^{(F3P)}$	$65^{(F3P)}$		
$2{,}88^{(CL)}$	$22^{(CL)}$	Southern Tunisia	[25]
$6^{(F3P)}$	$30^{(F3P)}$		

3.2.4. Fiber tensile test

Figure 15 shows the load-displacement curve of the trunk fiber tensile test Figure 14, noting that the curve at a linear rate up to a value of 39.8 N and displacement 0.5 mm, followed by a sudden break. These results are illustrated in Table 6.

Figure 14. Fiber tensile test bench

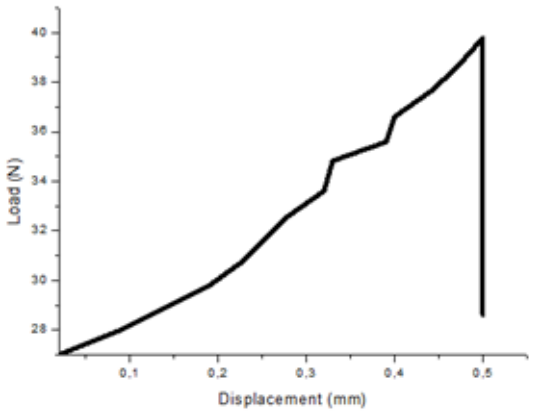

Figure 15. Load - Displacement Curve

Table 6. Results of the fiber tensile test

Max Load (N)	Max Stress (MPa)	Displacement (mm)	YOUNG'smodulus (MPa)
39.8	140.83	0.5	8801.87

Table 7. Comparison of the mechanical properties of date palm fibres

	Modulus of elasticity [GPa]	Max Stress [MPa]	Region	References
Date Palm	8.8	140.83	Bechar	Présente étude
	9,29–22,81	195,21–378,83	Biskra-Algeria	[27]
	6–11	180–320	Egypt	[15]
	2,5–12	97–275		[31]
	2–7,5	58–203		[24]
	8.8_6x10^{-3}	125,97	M'sila-Algérie	[19]

3.2.4. Fatigue test

The stress-number curve of cycles, shown in figure 19, is derived from the fatigue tests of figure 16. It begins at the limit of amplitude stress associated with a specific number of cycles until the rupture, σ d=99.58 N/mm2, and then extends to an infinite number of cycles under a light load. The results of the fatigue test are shown in Table 8, where the magnitude of the stress is proportional to the number of cycles.

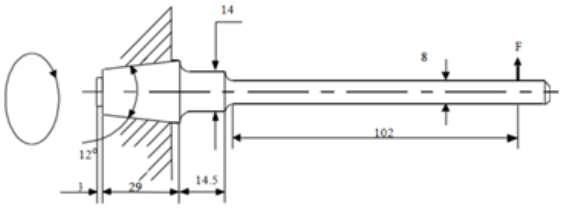

Figure16. Cyclic fatigue test bench, Figure17.Fatigue test specimen,Figure18. Test pieces after the fatigue test

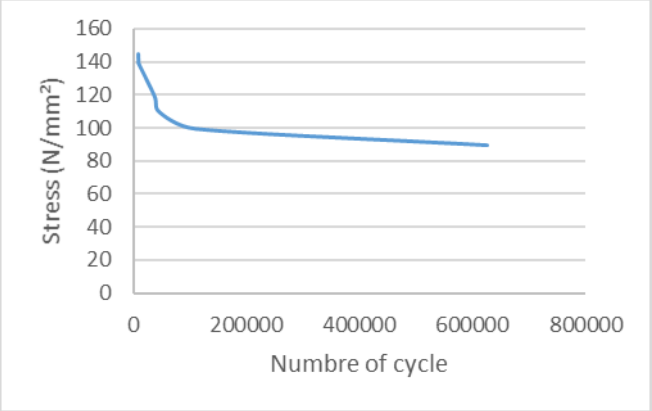

Figure 19. Stress - number of cycles curve (σa-Nr)

Table 8.Fatigue test result

Specimen N°	Charge F		σ_aN/mm²	Revolution
	Kg	N		
01	6.50	63.70	129.327	24983
02	6.00	58.90	119.582	65880
03	5.75	56.40	114.506	120101
04	5.50	53.95	109.532	248958
05	5.00	49.45	100.396	1000000

Sample performance curves

The results of the test, carried out on several test pieces, as shown in Figure 18, shall be represented in the form of a curve, σ-Nr. This curve expresses the relationship between amplitude constraint and number of cycles. It is commonly referred to as the Wöhler diagram, as illustrated in figure 19.

4. Conclusion

The objective of this study was to characterize and analyze the behavior of the trunk in both static and fatigue. First, we determined the physic-mechanical characteristics of this material, then the endurance limit.

The results obtained from the mechanical tests on various test pieces obtained from the trunk have revealed that the mechanical properties of the trunk, subjected to variable tensile loads according to the standard NF ISO 527, in compression whose fibres are orientated longitudinally and transversely according to the standard NF B51-007-ISO3132-1975, and in three-point bending according to the standard NF en ISO 178, only in the longitudinal direction of the fibres of the trunk, are acceptable. In addition, these results demonstrated a remarkable improvement in resistance, validated by comparison with tests carried out on date palm trunks from other regions.

Fatigue tests have shown that cracks can form in places where stress is high, and that they can remain invisible to the naked eye. When these cracks are subjected to repeated cyclic stresses, they propagate slowly, leaving the untracked part supported by the load. As a result, the untracked portion remains constantly under a higher stress until the occurrence of the final failure.

5. References

[1] N.Bouguedoura, A. Benkhalifa, M. Bennaceur, Situation, contraintes et apports de
[2] larecherche, le palmier dattier en Algérie 08 juin 2017.
[3] Memon A. &Nakai A. Mechanical Properties of Jute Spun Yarn/PLA Tubular
[4] Braided Composite by Pultrusion Molding, Energy Procedia, Vol 34, 818-829, 2013
[5] Baley C. &Bourmaud A., Average tensile properties of French elementary flax fibers, Materials Letters, Vol. 122, 159-161,2014
[6] Mahjoub R., Yatim J. M.,Mohd Sam A. R. &Hashemi S. H. Tensile properties
[7] ofkenaf fiber due to various conditions of chemical fiber surfacemodifications,
[8] Construction and Building Materials, Vol 55, 103–113,2014
[9] George M., Mussone P. G., Abboud Z. &Bressler C. D., Characterization of
[10] chemically and enzymatically treated hemp fibres using atomic force microscopy andspectroscopy, Applied Surface Science , Vol 314, 1019-1025, 2014
[11] Belaadi A., Bezazi A., Bourchak M. &Scarpa F. Tensile static and fatigue
[12] behaviour of sisal fibres, Materials and Design , Vol 46, 76-83, 2013
[13] Liu K, Zhang X., Takagi H., Yang Z. & Wang D. Effect of ChemicalTreatments on Transverse Thermal Conductivity of Unidirectional AbacaFiber/Epoxy Composite. Composites Part A: Applied Science and Manufacturing, Vol 66, 227-236,2014
[14] Chen D., Jing Li &JieRen. Influence of fiber surface-treatment on interfacial
[15] property of poly(l-lactic acid)/ramie fabric bio-composites under UV-irradiation
[16] hydrothermal aging, Materials Chemistry and Physics , Vol126, 524-531, 2011
[17] LeDuigou A, Davies P, Baley C. « Interfacial bonding of flax fiber/poly(L-lactide)
[18] bio-composites ». Composites Science and Technology. Vol. 70, pp. 231-239, 2010
[19] B.Agoudjil, A. Benchabane, A. Boudenne, L. Ibos, M. FoisMatériaux
[20] renouvelables pour réduire les déperditions thermiques du bâtiment:Caractérisation du bois de palmier dattier Énergie Construire, 43 (2-3) pp. 491 – 497. 2011
[21] Kandola B, Kandare E. Composites having improved fireresistance. In: Advances in Fire retardant materials, Elsevier; p. 398–442.2008
[22] Rout J, Misra M, Tripathy S, Nayak S, Mohanty A. Surfacemodification of coir fibers. II. Cu (II)-IO initiated graftcopolymerization of acrylonitrile onto chemically modifiedcoir fibers. J ApplPolymSci;84(1):75–82.2002
[23] FM AL-Oqla, OY Alothman, M. Jawaid, SM Sapuan, M. Es-SahebTraitement et
[24] propriétés des fibres de palmier dattier et de ses composites. La biomasse et la bioénergie, Springer, pp. 1 – 25. 2014
[25] MH Geith, MA Aziz, W. Ghori, N. Saba, M. Asim , M. Jawaid , et al.
[26] Propriétés mécaniques en flexion, thermique et dynamique des composites époxys
[27] renforcés de fibres de palmier dattier J Mater ResTechnol , 8 (1), pp. 853 – 860. 2019
[28] ME Ali, A. AlabdulkaremSur les caractéristiques thermiques et la microstructure
[29] d'un nouveau matériau isolant extrait des fibres de surface des palmiers dattiers

[30] Constr Mater Construire , 138, pp. 276 – 284. 2017
[31] M. K. Jahromi, A. Jafari, S. Mohtasebi, and S. Rafiee, "Engineering properties of date palm trunk applicable in designing a climber machine," Agricultural Engineering International: CIGR Journal, 2008.
[32] MustaphaBoumhaoutbLahcenBoukhattemcHassan Hamdi Brahim Benhamou Fatima Ait Nouh , Caractérisation thermomécanique d'un matériau de construction bio-composite : Mortier renforcé de treillis de fibres de palmier dattier , Matériaux de construction et de construction, Volume 135 , 15 mars 2017, Pages 241-250
[33] A.Gherfi , R. Belakroum , C. Maalouf , M. Lachi , A. MerabetCite web :https://www.researchgate.net/profile/GherfiAbdelhafid/publication/321421325_Permeabilite_a_la_vapeur_d'eau_d'un_composite_d'isolation_biosource_a_base_de_fibre_de_palmier_dattier/links/5dc8763ba6fdcc57503ddaae/Permeabilite-a-la-vapeur-deau-dun-composite-disolation-biosource-a-base-de-fibre-de-palmier-dattier.pdf
[34] Tarek Djoudi1, Mabrouk Hecini1, Daniel Scida3, Youcef Djebloun2, and Belhi Guerira1, Caractérisation physique et mécanique du bois etdes fibres issus d'une palme mûre de palmier dattier, Matériaux & Techniques 106, 403 (2018)
[35] K.Almi, A. Benchabane, S. Lakel, A. Kriker, Potential utilization of date palm wood as composite reinforcement, J. Reinforced Plas. Compos. 34, 1231 (2015)
[36] M.Baali, Contribution à la caracterisation et à l'exploration de la microstructure et des proprietes des constituants du palmier, Mémoire de magistere, Université Mohamed
[37] Khider-Biskra, Algérie, 2012
[38] E.S.Ellouze A, S. Medhioub, Détermination des caractéristiques mécaniques du bois tronc palmier, Séminaire International, INVACO2,Rabat-Maroc, no 30–123, novembre 2011
[39] E.A.Elbadry, Agro-Residues: Surface treatment and characterization of date palm tree fiber as composite reinforcement, Hindawi Publishing Corporation, J. Compos. 2014, Article ID 189128, 2014
[40] F.M. Al-Oqla, S. Sapuan, Natural fiber reinforced polymer composites in industrial applications: feasibility of date palm fibers for sustainable automotive industry, J. Clean. Prod. 66, 347 (2014)
[41] A.Alawar, A.M. Hamed, K. Al-Kaabi, Characterization of treated date palm tree fiber as composite reinforcement, Compos. Part B: Eng. 40, 601 (2009)
[42] A.Bezazi, S. Amroune, F. Scarpa, Analyse statistique et effet des traitements chimique sur le comportement physicomécanique des fibres des bras de grappe des palmiers dattier,
[43] Synthèse : Revue Sci. Technol. UBMA 31, 108 (2015)
[44] TarekDjoudi, Mabrouk Hecini, and all, Caractérisation physique et mécanique du bois et
[45] des fibres issus d'une palme mûre de palmier dattier, Matériaux & Techniques 106, 403 (2018)